Evolution of the resonances of two parallel dielectric cylinders with distance between them

E. N. Bulgakov,[1,2] K. N. Pichugin,[1,2] and A. F. Sadreev ®[1]

[1]*Kirensky Institute of Physics, Federal Research Center KSC Siberian Branch, Russian Academy of Sciences, Krasnoyarsk 660036, Russia*
[2]*Reshetnev Siberian State University of Science and Technology, Krasnoyarsk 660037, Russia*

We study evolution of resonant modes by traversing over the distance between two parallel dielectric cylinders. The processes of mutual scattering of Mie resonant modes by cylinders result in an interaction between the cylinders which lifts a degeneracy of resonances of the isolated cylinders. There are two basic scenarios of evolution. For strong interaction of cylinders resonances bypass the Mie resonances with increase of the distance. That scenario is typical for low-lying resonances (monopole and dipole). For weak interaction of cylinders the resonances are bound around the Mie resonances of isolated cylinders that form the second scenario. Both scenarios demonstrate a significant enhancement of the Q factor compared to the case of an isolated cylinder.

I. INTRODUCTION

It is rather challenging for optical resonators to support resonances of simultaneous subwavelength mode volumes and high Q factors. The traditional way for increasing the Q factor of optical cavities is a suppression of leakage of the resonance mode into the radiation continua. That is achieved usually by decreasing the coupling of the resonant mode with the continua by the use of metals, photonic band gap structures, or whispering-gallery-mode resonators. All of these approaches lead to reduced device efficiencies because of complex designs, inevitable metallic losses, or large cavity sizes. On the contrary, all-dielectric subwavelength nanoparticles have recently been suggested as an important pathway to enhance capabilities of traditional nanoscale resonators by exploiting the multipolar Mie resonances being limited only by radiation losses [1,2].

The decisive breakthrough came with the paper by Friedrich and Wintgen [3], which put forward the idea of destructive interference of two neighboring resonant modes leaking into the continuum. Based on a simple generic two-level model they formulated the condition for the bound state in the continuum (BIC) as the state with zero resonant width for crossing of eigenlevels of the cavity or avoided crossing of resonances. This principle was later explored in an open plane wave resonator where the BIC occurs in the vicinity of degeneracy of the closed integrable resonator [4].

However, these BICs exist provided that they embedded into a single continuum of propagating modes of a directional waveguide. In photonics the optical BICs embedded into the radiation continuum can be realized in two ways. The first way is realized in an optical cavity coupled with the continuum of 2D photonic crystal (PhC) waveguide [5] that is an optical variant of the microwave system [4]. An alternative way is the use of periodic PhC systems (gratings) or arrays of dielectric particles in which resonant modes leak into a restricted number of diffraction continua [6–10]. Although the exact BICs can exist only in infinite periodical arrays [11,12], finite arrays demonstrate resonant modes with the very high Q factor which grows quadratically [13] or even cubically

[14] with the number of particles (quasi-BICs). Even arrays of three [15] and five dielectric rods demonstrate the Q factor exceeding the Q factor of an individual particle by two and six orders in magnitude, respectively [16].

Isolated subwavelength high-index dielectric resonators are more advantageous from an applied point of view to achieve high Q resonant modes (supercavity modes) [2,17,18]. Such supercavity modes originate from avoided crossing of the resonant modes, specifically the Mie-type resonant mode and the Fabry-Pérot resonant mode under variation of the aspect ratio of the dielectric disk which could result in a significant enhancement of the Q factor. It is worthy also to notice the idea of formation of long-lived, scarlike modes near avoided resonance crossings in optical deformed microcavities [19]. The dramatic Q factor enhancement was predicted by Boriskina [20,21] for avoided crossing of very high-lying whispering gallery modes in symmetrical photonic molecules of dielectric disks on a surface.

In the present paper we study evolution of resonances of two parallel dielectric cylinders under variation of distance between them as sketched in Fig. 1 with a focus on the Q factor. We consider the avoided crossing of low-lying resonant modes (monopole, dipole, and quadruple) as different from papers in [19–25], where the avoided crossing of high-lying resonances, whispering gallery modes were considered.

II. AVOIDED CROSSING UNDER VARIATION OF DISTANCE BETWEEN TWO CYLINDERS

The problem of scattering of electromagnetic waves from two parallel infinitely long dielectric cylinders sketched in Fig. 1 was solved a long time ago [26–28]. The solutions for the electromagnetic field for the TE polarization with the component of electric field directed along the cylinders $\psi = E_z$ (see Fig. 1) outside the cylinders are given by series over the Hankel functions

$$\psi_1 = \sum_n A_{1n} H_n^{(1)}(kr_1) e^{in\theta_1}, \tag{1}$$

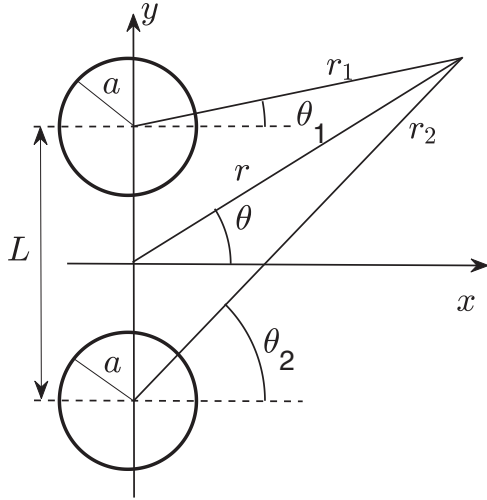$$\psi_2 = \sum_n A_{2n} H_n^{(1)}(kr_2) e^{in\theta_2}. \tag{2}$$

043806-1

FIG. 1. Two identical infinitely long parallel dielectric cylinders with radii a and refractive index $\sqrt{\epsilon} = \sqrt{30}$.

Inside the cylinders the solution is given by series over the Bessel functions

$$\psi_1 = \sum_n B_{1n} J_n(\sqrt{\epsilon} k r_1) e^{in\theta_1}, \tag{3}$$

$$\psi_2 = \sum_n B_{2n} J_n(\sqrt{\epsilon} k r_2) e^{in\theta_2}. \tag{4}$$

By means of the Graf formula [29]

$$H_n^{(1)}(kr_1) e^{in\theta_1} = \sum_m i^{n-m} H_{m-n}^{(1)}(kL) J_m(kr_2) e^{im\theta_2}, \tag{5}$$

$$H_n^{(1)}(kr_2) e^{in\theta_2} = \sum_m i^{n-m} H_{m-n}^{(1)}(kL) J_m(kr_1) e^{im\theta_1}, \tag{6}$$

the total field $\psi = \psi_1 + \psi_2$ can be written completely in either coordinate system.

Applying the boundary conditions at $r_j = a$ leads to the system of homogeneous algebraic equations [26,28]

$$
\begin{aligned}
A_{1n} &= i^n S_n(k) \sum_m i^{-m} H_{n+m}(kL) A_{2n}, \\
A_{2n} &= i^n S_n(k) \sum_m i^{-m} H_{n+m}(kL) A_{1n},
\end{aligned}
\tag{7}
$$

where S_n are the scattering matrix amplitudes for the isolated cylinder

$$S_m(k) = \frac{\sqrt{\epsilon} J'_m(\sqrt{\epsilon} ka) J_m(k) - J'_m(k) J_m(\sqrt{\epsilon} k)}{H_m^{(1)'}(k) J_m(\sqrt{\epsilon} k) - \sqrt{\epsilon} J'_m(\sqrt{\epsilon} k) H_m^{(1)}(k)}. \tag{8}$$

The solutions of this system (7) define the resonant modes if

$$\mathrm{Det}[\hat{M}^2 - I] = 0 \tag{9}$$

or

$$\mathrm{Det}[\hat{M} \pm I] = 0, \tag{10}$$

where the sign "$\pm$" responds for antisymmetric and symmetric resonances, respectively. The complex roots of these equations define the resonant frequencies or poles of the S matrix, where matrix elements $\hat{M}$ are given by Eq. (7) and
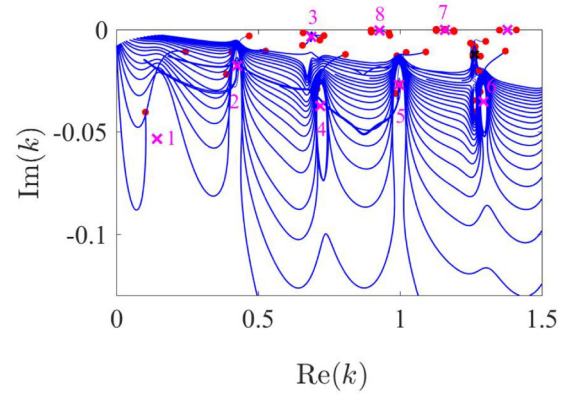

FIG. 2. Evolution of resonances (poles) with the distance between cylinders. Closed circles correspond to minimal distance $L = 2a$, where a is the radius of cylinders and crosses mark the indexed Mie resonant frequencies of the isolated cylinder shown in Fig. 3.

equal

$$M_{mn} = S_m(k) i^{m-n} H_{m+n}(kL) \tag{11}$$

and I is the unit matrix.

Rigorously speaking the rank of the matrix $\hat{M}$ given by the number of the azimuthal indices m in series (7) is infinite. However, in practice for numerical computation of the resonant frequencies we have to restrict the rank of the matrix $\hat{M}$ where the choice of the rank is determined by the range of resonant frequencies in which we are interested. In the present paper we are restricted by the case of subwavelength cylinders $ka \sim 1$ for which the rank defined by inequality $-5 \leqslant m \leqslant 5$ turns out sufficient. In Fig. 2 we show the results of computation or complex roots of Eq. (10) in the form of their evolution for traversing over L. To simplify the picture we presented only a part of the resonant frequencies. First of all one can see from Fig. 2 that a major part of the resonances evolves with the distance by-passing the Mie resonances of the isolated cylinder marked by crosses. Second, there is a small part of the resonances which are bound around the Mie resonances with small imaginary parts. As a rule these Mie resonances correspond to high-lying Mie resonances.

Let us consider the asymptotic behavior of poles for $L \to \infty$. By use of asymptotical behavior of the Hankel functions [30] we have for matrix (11) the following:

$$M_{mn} \sim \sqrt{\frac{2}{\pi k L}} e^{i(kL - \pi/4)} S_m(k) (-1)^n. \tag{12}$$

Let us take the eigenvector of matrix $\hat{M}$ $\vec{\psi}^+ = (\psi_1, \psi_2, \psi_3, \ldots)$. Then Eq. (9) takes the following form:

$$\sqrt{\frac{2}{\pi k L}} e^{ikL} S_m(k) \sum_n (-1)^n \psi_n = \pm \psi_m, \tag{13}$$

which has the solution provided that

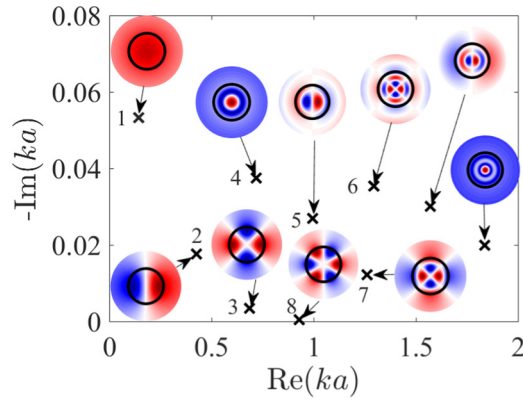$$\sqrt{\frac{2}{\pi k L}} e^{ikL} \sum_n (-1)^n S_n(k) = \pm 1. \tag{14}$$

FIG. 3. Dimensionless Mie resonances (close circles) and corresponding resonant modes (the component E_z) of the isolated cylinder.

For the absolute value we have

$$\frac{2e^{2\gamma_n L}}{\pi |k_n| L} = \frac{1}{|\sum_m (-1)^m S_m(k_n)|^2}, \tag{15}$$

where $\gamma_n = -\text{Im}(k_n)$. The poles of the isolated cylinder are given by the poles of the S matrix, i.e., by equation $S_m(k_n)^{-1} = 0$. Therefore, from (15) it follows that, first, the poles of double cylinders do not converge to the poles of the isolated cylinder at $L \to \infty$. The reason is related to the exponential factor $\exp(\gamma_n L)$ of the resonant modes. In open systems an eigenmode acquires a certain linewidth or finite lifetime, so that the eigenfrequency becomes complex valued due to leakage to the outside of cylinders. In the literature these are also known as Gamow states [31] or leaky modes [32]. Second, although $k_n \to 0$ at $L \to \infty$ as indeed Figs. 4(a) and 4(b) illustrate, the factor $\text{Im}(k_n L)$ shown in Fig. 4(c) diverges to a result in a divergence of the resonant modes at large distances L that constitutes the problem with normalization of the resonant modes [33].

Next, we consider the behavior of some typical resonances shown in Fig. 2. Due to the symmetry relative to $x \to -x$ and $y \to -y$ the resonant modes can be classified as $\psi_{\sigma,\sigma'}$, where the indices $\sigma = s, a$ respond for symmetric and antisymmetric modes, respectively [22]. We start with the first two lowest symmetric and antisymmetric resonances whose evolution is shown in Fig. 5(a). One can see that the resonant modes outside the cylinders can be approximated as hybridizations

FIG. 5. Evolution of resonant frequencies and monopole modes $\psi_{s,s/a}^{(0)}$ (a) and the Q factors with the distance between the cylinders. Solid (dash) line shows symmetric (antisymmetric) resonances. Closed circles correspond to $L = 2a$, open circles correspond to $L = 1000a$, and cross corresponds to the monopole Mie resonance 1.

of the Mie resonant modes

$$\psi_{s;s/a}^{(m)} = H_m^{(1)}(kr_1)\sin(m\theta_1) \pm H_m^{(1)}(kr_2)\sin(m\theta_2),$$
$$\psi_{a;s/a}^{(m)} = H_m^{(1)}(kr_1)\cos(m\theta_1) \pm H_m^{(1)}(kr_2)\cos(m\theta_2), \tag{16}$$

with $m = 0$, i.e., monopole Mie resonances except for the close distance between the cylinders. Figure 5(b) shows the evolution of the Q factor $Q = -\text{Re}(k_n)/2\,\text{Im}(k_n)$ for both resonances. The Q factor of the antisymmetric resonance at $L = 2a$ exceeds the Q factor of the isolated cylinder as well as the Q factor of the symmetric resonance by one order in magnitude. As seen from Fig. 5(a) the antisymmetric resonant mode becomes the dipole mode at $L = 2a$, which has the resonant width by one order less than the resonant width of the monopole mode as seen from Fig. 3.

The next resonances refer to hybridizations of the Mie dipole, quadruple, etc. resonances which are degenerate in the isolated cylinder. The coupling between cylinders strongly depends on the symmetry of Mie resonant modes. The general expressions and physical origin of the coupling of dielectric resonators was considered in Refs. [34–36]. The coupling constant can be written as [35]

$$v = \int dx\, dy [\epsilon(\vec{r}) - 1]\vec{E}_1^{*}\vec{E}_2, \tag{17}$$

where $\vec{E}_{1,2}$ are normalized solutions. Here the indices 1 and 2 imply the resonant modes of isolated cylinders. One can
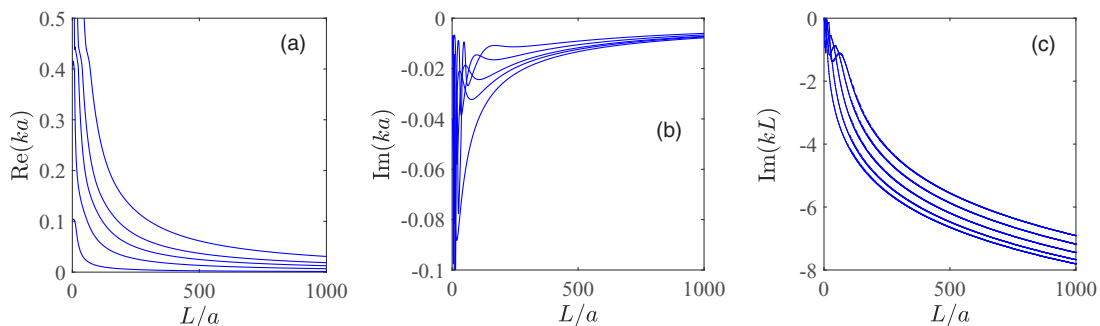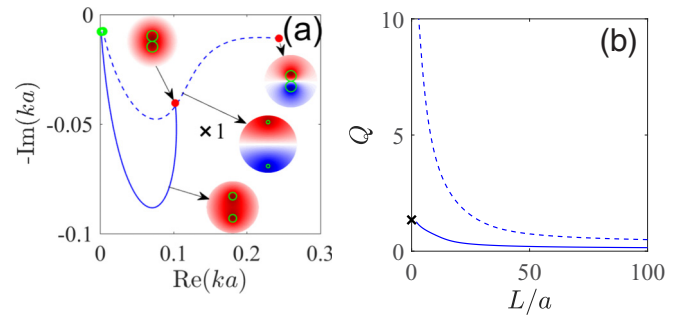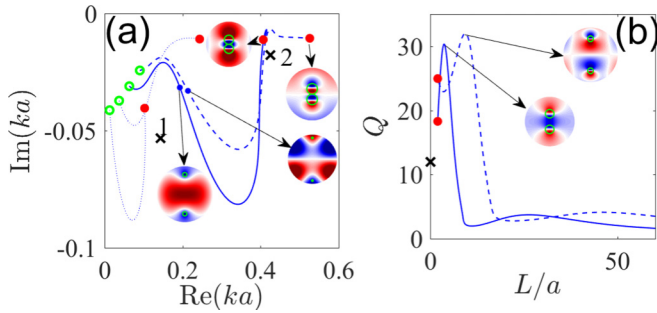

FIG. 4. Behavior of resonant positions (a), resonant widths (b), and imaginary parts $\text{Im}(kL)$ (c) of a few lowest resonances shown in Fig. 2 on the distance between cylinders.

FIG. 6. Same as in Fig. 5 for hybridization of the Mie dipole resonant modes. Cross marks the Q factor of the isolated cylinder.

FIG. 8. Example of the evolution of the symmetric resonances from the Mie resonance 4 (a) and 5 (b).

see that the coupling constant is determined by overlapping of resonant Mie modes which in turn depend on a distance between the particles and directivity of radiation of the Mie resonant mode.

That conclusion is well illustrated by the Mie dipole resonant modes which are degenerate. The first dipole Mie resonant mode, symmetric relative to $x \to -x$, radiates prevalently towards the neighboring cylinder as shown in insets in Fig. 6, while the second antisymmetric dipole Mie resonant mode radiates away from the neighboring cylinder as shown in insets of Fig. 7. As a result the interaction in the former case turns out stronger compared to the latter case as it follows from Eq. (17). That explains why the evolution of resonances shown in Fig. 6(a) is similar to the case of interaction via the monopole resonant modes in Fig. 5, while the evolution of resonances in Fig. 7(a) is bound to the Mie dipole resonance 2. Respectively, the gain in the Q factor in the former case is smaller than in the latter case as seen from Figs. 6(b) and 7(b).

Moreover, for the symmetric resonance $\psi_{s;s/a}^{(1)}$ the coupling between the cylinders is so strong that resonance bypasses the Mie dipole resonance 2 and then bypasses the monopole Mie resonance 1 becoming close to the monopole resonance $\psi_{s;s}^{(01)}$. That property of symmetric hybridizations to bypass one by one the Mie resonances is brightly illustrated in Fig. 8, where at each event the resonant mode inside the cylinders becomes close to the respective Mie resonant modes. Figures 8(a) and 8(b) illustrate evolution of the resonances from the Mie resonances 4 and 5, respectively. As shown in Fig. 3 they correspond to the monopole and dipole Mie resonant modes

with higher eigenfrequencies because of the nodal radial line. Therefore, the coupling (17) is weakened compared to the monopole and dipole resonances 1 and 2, respectively. As a result for traversing over the distance from the shortest distance $L = 2a$ till $L \approx 10a$ the resonances are bound to the corresponding Mie resonances as seen from Figs. 8(a) and 8(b). However, with further increase of distance the coupling between cylinders increases because of exponential factor $\exp(\gamma_n L)$, where $n = 4, 5$. That unbinds the resonances from the original Mie resonances 4 and 5, which bypass the low-lying Mie resonances one by one.

For the antisymmetric resonance $\psi_{a;s/a}^{(1)}$ the evolution is cardinally different as shown in Fig. 7(a). When the cylinders are close to each other the coupling is maximal, which results in the maximal repulsion of the resonant frequencies. A separation of the cylinders weakens the coupling so that the resonances, symmetric and antisymmetric, are both bound to the dipole Mie resonance 2 in Fig. 7(a). However, with further separation of cylinders the coupling is strengthened because of growth of the exponential contribution $\exp(2\gamma_2 L)$, however small the resonant width γ_2 was. As the result, the resonant trajectories are unbound when the distance exceeds $1/\gamma_1$. Figure 7(a) and forthcoming figures brightly illustrate this feature related to the exponential contribution $\exp(\gamma_n L)$ of resonant modes. Figures 9 and 10 illustrate the second scenario of evolution of resonances which are bounded by the quadruple, octuple, etc. Mie resonances of the isolated cylinder because of weakness of interaction of cylinders through these resonant modes. A spiralling of the complex resonant frequencies in 3D plots is a consequence of exponential contribution $\exp ikL$ in the asymptotic of Hankel functions. Respectively, we observe only oscillating behavior of the Q factor with substantial enhancement compared to the isolated cylinder. Figures 10(c) and 10(d) show that the Q factor can reach extremal enhancement for variation of the distance similar to the WGM resonances [19–21]. And similar to the dipole resonant hybridizations the evolution of hybridized resonances with $m = 2, 3, \ldots$ also crucially depends on the symmetry of the Mie resonant modes.

III. SUMMARY OF RESULTS AND CONCLUSIONS

For the isolated dielectric cylinder we have well known Mie resonances specified by azimuthal index $m = 0, \pm 1, \pm 2, \ldots$ (monopole, dipole, quadruple, etc. resonances) due to axial symmetry. Two parallel cylinders have no axial symmetry and therefore the solutions of homogeneous
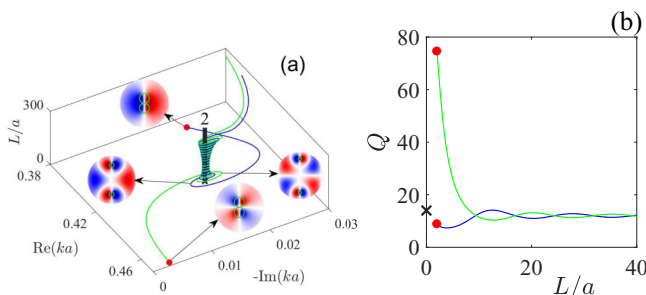

FIG. 7. Behavior of resonant modes, symmetric and antisymmetric hybridizations (16) of dipole resonant modes of isolated cylinders (a), and respective Q factors (b) for variation of distance between them. The dipole Mie resonance is shown by red cross.
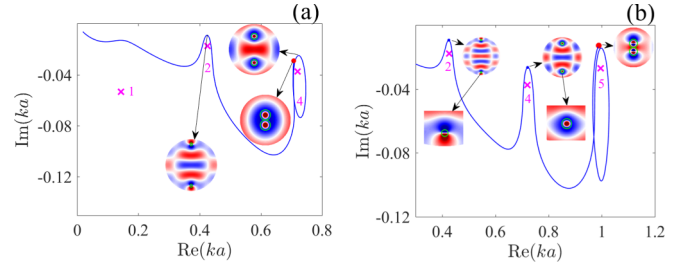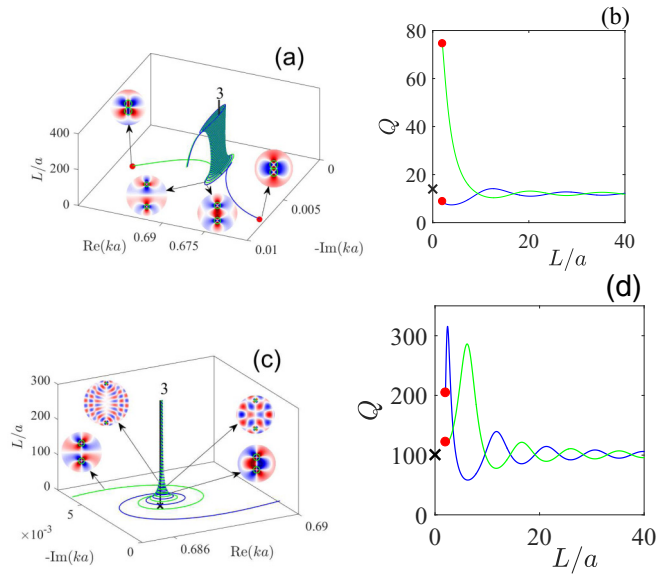
FIG. 9. (a), (c) 3D plots of resonant frequencies complimented by insets of resonant modes which are the hybridizations of the Mie quadruple resonant modes for traversing over L. Cross marks the quadruple Mie resonance 3 shown in Fig. 3. (b), (d) The corresponding behavior of the Q factors where red closed circles mark the case $L = 2a$.
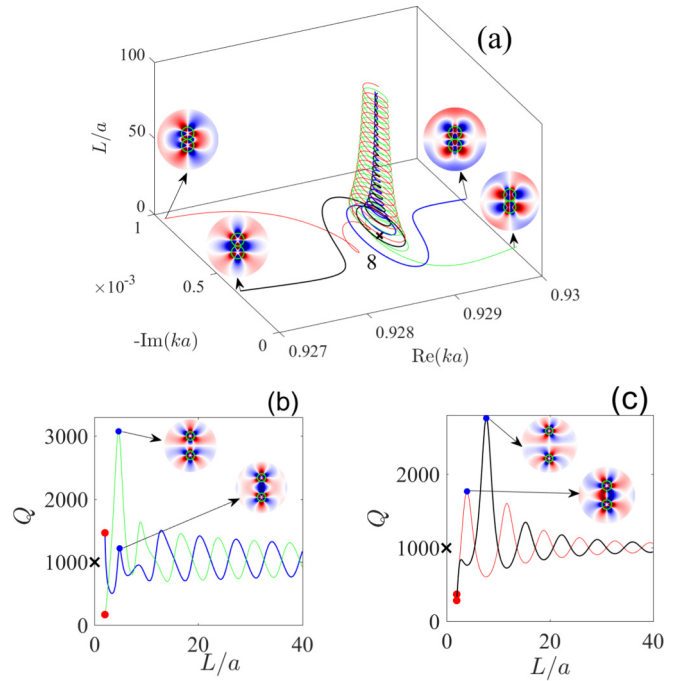

FIG. 10. (a) 3D plot of the octuple resonances with resonant modes in insets where cross marks the Mie resonance 8 shown in Fig. 3. (b),(c) The corresponding plots of Q factor vs the distance between cylinders.

Maxwell equations are given by a series of the Bessel (inside) or Hankel (outside cylinders) functions in m. However, there were no studies of the behavior of resonances of two identical cylinders dependent on distance between the cylinders except studies of the Q factor by Boriskina for extremely high-lying resonances, whispering gallery modes [20,21]. The study presented in this paper reveals surprisingly complicated behavior of the resonances with the distance which can be divided into two families. In the first family the resonances bypass the Mie resonances. At each event of that the resonant mode inside the cylinders takes the field profile of the corresponding Mie resonant mode, while the solution between the cylinders takes regular symmetric or antisymmetric packing of half wavelengths. At these moments the Q factor achieves maximal magnitudes. The resonances bound to the Mie resonances form the second family and typical for higher resonances with $m = 1, 2, 3, \ldots$.

The dipole Mie resonances are double degenerate in the isolated cylinder and constitute an exceptional case. Approach of the second cylinder lifts this degeneracy that plays an important role in the evolution of resonances with the distance. Those Mie resonant modes which radiate towards the neighboring cylinder give rise to the coupling between cylinders (17) larger than in the case of the Mie dipole resonant mode radiating away from the cylinder. As a result the resonances in

the first case bypass the Mie resonances, while in the second case resonances are bound. For variation of the distance the Q factor shows the highest values when the resonances bypass the Mie resonances, while in the second family the Q factor shows oscillating behavior with maxima which can exceed the Q factor of the isolated cylinder three times.

One can consider the evolution of resonances hybridized from the Mie resonant modes with the TM polarization (H modes) for traversing over the distance between cylinders. The corresponding system of algebraic equations for expansion coefficients is derived by Olaofe [26]. However, a consideration of the case of TM polarization brings little new compared to the case of TE polarization. It is worthy also to note that Olaofe has shown also oscillatory behavior of the cross section with cylinder separation L that was revisited recently by Dmitriev and Rybin [37].

[1] A. Kuznetsov, A. Miroshnichenko, M. Brongersma, Y. Kivshar, and B. Luk'yanchuk, Science **354**, aag2472 (2016).

[2] K. Koshelev, A. Bogdanov, and Y. Kivshar, Sci. Bull. **64**, 836 (2019).

[3] H. Friedrich and D. Wintgen, Phys. Rev. A **32**, 3231 (1985).

[4] A. F. Sadreev, E. N. Bulgakov, and I. Rotter, Phys. Rev. B **73**, 235342 (2006).

[5] E. N. Bulgakov and A. F. Sadreev, Phys. Rev. B **78**, 075105 (2008).

[6] S. P. Shipman and S. Venakides, Phys. Rev. E **71**, 026611 (2005).

[7] D. C. Marinica, A. G. Borisov, and S. V. Shabanov, Phys. Rev. Lett. **100**, 183902 (2008).

[8] C. W. Hsu, B. Zhen, J. Lee, S. G. Johnson, J. D. Joannopoulos, and M. Soljačić, Nature (London) **499**, 188 (2013).

[9] E. N. Bulgakov and A. F. Sadreev, Phys. Rev. A **90**, 053801 (2014).

[10] E. N. Bulgakov and A. F. Sadreev, Phys. Rev. A **96**, 013841 (2017).

[11] D. Colton and R. Kress, *Inverse Acoustic and Electromagnetic Scattering Theory*, 2nd ed. (Springer, Berlin, 1998).

[12] M. G. Silveirinha, Phys. Rev. A **89**, 023813 (2014).

[13] Z. F. Sadrieva, M. A. Belyakov, M. A. Balezin, P. V. Kapitanova, E. A. Nenasheva, A. F. Sadreev, and A. A. Bogdanov, Phys. Rev. A **99**, 053804 (2019).

[14] E. N. Bulgakov and A. F. Sadreev, Phys. Rev. A **99**, 033851 (2019).

[15] Q. H. Song and H. Cao, Phys. Rev. Lett. **105**, 053902 (2010).

[16] A. Taghizadeh and I.-S. Chung, Appl. Phys. Lett. **111**, 031114 (2017).

[17] M. V. Rybin, K. L. Koshelev, Z. F. Sadrieva, K. B. Samusev, A. A. Bogdanov, M. F. Limonov, and Y. S. Kivshar, Phys. Rev. Lett. **119**, 243901 (2017).

[18] A. Bogdanov, K. Koshelev, P. Kapitanova, M. Rybin, S. Gladyshev, Z. Sadrieva, K. Samusev, Y. Kivshar, and M. F. Limonov, Adv. Photon. **1**, 016001 (2019).

[19] J. Wiersig, Phys. Rev. Lett. **97**, 253901 (2006).

[20] S. V. Boriskina, Opt. Lett. **31**, 338 (2006).

[21] S. Boriskina, Opt. Lett. **32**, 1557 (2007).

[22] J.-W. Ryu, S.-Y. Lee, C.-M. Kim, and Y.-J. Park, Phys. Rev. A **74**, 013804 (2006).

[23] J. Unterhinninghofen, J. Wiersig, and M. Hentschel, Phys. Rev. E **78**, 016201 (2008).

[24] C. Schmidt, A. Chipouline, T. Käsebier, E.-B. Kley, A. Tünnermann, T. Pertsch, V. Shuvayev, and L. I. Deych, Phys. Rev. A **80**, 043841 (2009).

[25] M. Benyoucef, J.-B. Shim, J. Wiersig, and O. G. Schmidt, Opt. Lett. **36**, 1317 (2011).

[26] G. O. Olaofe, Radio Sci. **5**, 1351 (1970).

[27] J. W. Young and J. C. Bertrand, J. Acoust. Soc. Am. **58**, 1190 (1975).

[28] T.-G. Tsuei and P. W. Barber, Appl. Opt. **27**, 3375 (1988).

[29] K. Yasumoto and H. Jia, in *Electromagnetic Theory and Applications for Photonic Crystals*, edited by K. Yasumoto (MIT Press, Cambridge, MA, 2006), pp. 527–579.

[30] M. Abramowitz and I. A. Stegun, *Handbook of Mathematical Functions* (National Bureau of Standards, Gaithersburg, MD, 1964).

[31] G. Gamow, Z. Phys. **51**, 204 (1928).

[32] E. A. Muljarov, W. Langbein, and R. Zimmermann, Europhys. Lett. **92**, 50010 (2010).

[33] P. Lalanne, W. Yan, K. Vynck, C. Sauvan, and J.-P. Hugonin, Laser Photon. Rev. **12**, 1700113 (2018).

[34] I. Awai and Y. Zhang, Electron. Commun. Jpn. 2 Electron. **90**, 11 (2007).

[35] S. Y. Elnaggar, R. J. Tervo, and S. M. Mattar, J. Appl. Phys. **118**, 194901 (2015).

[36] A. Tayebi and S. Rice, arXiv:1812.10057v1.

[37] A. A. Dmitriev and M. V. Rybin, Phys. Rev. A **99**, 063837 (2019).